Analysis of Operational Factors Contributing to Aircraft Overflight Noise Variation

Melissa Lepe *
University of California Irvine, Irvine, CA, 92617, USA

Brandon Hadfield †, Marek Homola‡
Massachusetts Institute of Technology, Cambridge, MA, 02139, USA

Trinity Lee §
University of California Irvine, Irvine, CA, 92617, USA

Clement Li ¶, Phillip Hood‖
Massachusetts Institute of Technology, Cambridge, MA, 02139, USA

Jacqueline Huynh **
University of California Irvine, Irvine, CA, 92617, USA

R. John Hansman††
Massachusetts Institute of Technology, Cambridge, MA, 02139, USA

Significant variations in measured overflight noise is observed from airport monitor networks, even for similar aircraft flying comparable operational procedures. Operational factors including aircraft configuration, acceleration and deceleration procedures, thrust profiles and associated environmental factors, can impact noise. To assess these impacts, operational Automatic Dependent Surveillance–Broadcast surveillance and weather data were associated with noise monitor recordings for a three-year period at Seattle-Tacoma and John Wayne International Airports, for Boeing 737-800, Boeing 737-700, and Airbus A320 aircraft. The impact of flight procedures on noise observations are assessed by evaluating flight profiles by airline to investigate the impact of differences in departure and arrival procedure. It was observed that aircraft

*Graduate Student, Samueli School of Engineering, 4200 Engineering Gateway, AIAA Student Member; lepem@uci.edu
†Graduate Student, Department of Aeronautics and Astronautics, 77 Massachusetts Ave., AIAA Student Member.
‡Graduate Student, Department of Aeronautics and Astronautics, 77 Massachusetts Ave., AIAA Student Member.
§Graduate Student, Samueli School of Engineering, 4200 Engineering Gateway, AIAA Student Member
¶Postdoc, Department of Aeronautics and Astronautics, 77 Massachusetts Ave., AIAA Member.
‖Undergraduate Student, Department of Aeronautics and Astronautics, 77 Massachusetts Ave., AIAA Student Member.
**Assistant Professor, Samueli School of Engineering, 4200 Engineering Gateway, AIAA Member.
††Professor, Department of Aeronautics and Astronautics, 77 Massachusetts Ave., AIAA Fellow.
Presented as Paper 2025-2005 Multifactor Analysis of Operational Factors Contributing to Aircraft Overflight Noise Variation at the AIAA SciTech 2025 Forum, Orlando, FL, January 9, 2025

weight and thrust correlate positively with noise on departure. At John Wayne Airport, there is evidence that thrust variations can result in large differences in noise near the airport while procedural differences, such as a steeper initial climb seen at both airports, can reduce noise levels at further distances. Noise on arrival was observed to correlate more closely with airspeed and shows evidence of being dependent on aircraft flap configuration.

I. Nomenclature

$ADS-B$	=	Automatic Dependent Surveillance–Broadcast
AL	=	Airline
avg	=	Average
$BADA$	=	Base of Aircraft Data
C_L	=	Lift Coefficient
$C_{L,Max}$	=	Maximum Lift Coefficient
dB	=	Decibels
deg	=	Degree
eng	=	Engine
ft	=	Feet
K	=	Kelvin
$KTAS$	=	Knots True Airspeed
km	=	Kilometers
kts	=	Knots
lb	=	Pounds
m	=	Meters
$MTOW$	=	Maximum Takeoff Weight
nmi	=	Nautical Miles
No	=	Number
OEW	=	Operating Empty Weight
p	=	Atmospheric Pressure
s	=	Seconds
S	=	Wing Surface Area
SEL	=	Sound Exposure Level
TOW	=	Takeoff Weight
V	=	Velocity

$V_{approach}$ = Aircraft Approach Speed

V_{Ground} = Aircraft Ground Speed

V_{Ind} = Indicated Airspeed

V_{REF} = Reference Landing Speed

V_{Stall} = Stall speed

V_{True} = True Airspeed

V_{Wind} = Atmospheric Wind Speed

V_2 = Takeoff Safety Speed

u = Eastward Winds

v = Northward Winds

z = Altitude

β = Regression Coefficients

ΔV_2 = Departure Speed Margin

δ_f = Flap Setting

ρ = Density

II. Introduction

Aviation-caused community noise due to departing and arriving aircraft remains a significant environmental challenge around airports. Field measurements of noise from overflight events around airports have historically shown significant variations (on the order of 10 dB) [1, 2] in noise levels, even for flights using the same aircraft type flying similar trajectories. This variation has traditionally been attributed to factors such as varied thrust levels, aircraft configuration and propagation effects however there have been limited direct investigations into the procedural causes of this variation. Understanding these causes can provide insight for overflight noise mitigation strategies, such as noise abatement procedures, and could also be used to inform future refinements of aircraft noise models, such as NASA's Aircraft NOise Prediction Program (ANOPP) [3] or the Federal Aviation Administration (FAA)'s Aviation Environmental Design Tool (AEDT) [4].

Airport noise monitor networks can be utilized to examine aircraft noise effects. Such networks are often placed

around airports to continuously monitor noise levels of aircraft departure and arrival procedures. Normally airport operators correlate noise observations with associated flights but do not have access to the detailed aircraft states for those flights. For example, [5] presents a method to decouple sources of noise originating from aircraft and those originating from non-aircraft sources in airport noise measurements using surveillance data.

Correlating surveillance data with measured noise and weather data has also been used to validate or assess procedural effects on noise, such as in approach noise assessments [2, 6]. In addition, recent applications of trajectory clustering from surveillance data have been used to identify specific patterns in flight procedures [7], which can also be related to noise levels.

Noise recordings have been investigated to identify patterns in procedure and operational conditions using a variety of techniques. One technique is using machine learning to predict a flight's noise footprint with available data. For example, [8] developed machine learning models to assess aircraft noise from more detailed aircraft noise models, and Toraman et al. [9] developed models to predict noise levels on approach and departure from a limited number of factors, such as thrust and weight. The engine thrust and weight estimates using the Aircraft Noise and Performance database [10] along with meteorological information, is used in [11] to also predict approach and departure noise. In [12–14] the authors use a convolutional-neural network architecture to predict airport noise emissions of aircraft, but remove the effects of other sources. Further efforts to predict noise have used strategies such as supervised learning [15], or physics based neural networks [16] to predict noise at a monitor based on the operating conditions.

In most of these techniques, noise is typically evaluated as a single noise monitor and correlated with aircraft states and other factors. An example is in [1], where linear regression was used to identify correlations between factors and noise at single monitors. These methods provide some insight but do not capture effects of the full flight procedure where flight trajectory and actions prior to monitor passing may influence the observed noise.

Methods for considering full flight procedures were presented in [7, 17, 18], where hierarchical clustering was applied in to identify procedural and operational differences in flight trajectories. This method clustered operational behaviors hierarchically using K means techniques resulting in similarity in lateral position, speed, vertical rate, and thrust. Preliminary findings showed that some of the identified clusters were almost entirely composed of a single airline, indicating a strong relationship between airline and trajectories similarity presumably due to airline specific operational procedures. Consequently, a comparative analysis by individual airline is included in this study to help

identify the impact of varied operational procedures.

The airline comparative analysis presented here is conducted using noise monitor data from two airports, Seattle-Tacoma International Airport (SEA) and John Wayne Airport (SNA), for departing and arriving Boeing 737-700, Boeing 737-800, and Airbus A320 aircraft. Airline departure and arrival trajectories are grouped to identify how airline specific procedures and other factors influence noise level along the monitors under the flight trajectories. Automatic Dependent Surveillance–Broadcast (ADS-B) surveillance data is used directly observe trajectory factors, such as position, altitude, and ground speed. Airspeed is derived from the observed ground speed corrected for wind from meteorological models. Aircraft weight is not available directly from the ADS-B data but is derived from initial and final stable airspeeds or from airline reported data, when available. Thrust is derived from a simple dynamics model based on the assumed weights and observed trajectory states.

The remainder of the paper is structured as follows. Section III presents the data sources and methodology used to relate noise to operational factors, including descriptions of the airline-based analysis approach. Section IV demonstrates an implementation of these methods at Seattle-Tacoma International Airport (SEA) and John Wayne Airport (SNA) and observations of procedural or operational factors which influence noise levels are discussed. Finally, conclusions of the results obtained across airports are discussed in Section V.

III. Method for Relating Noise Variation to Operational Factors

This section presents the method of reconstructing details of the aircraft states from publicly available surveillance data and correlating with noise monitor data.

A. Data Sources

1. Seattle-Tacoma International Airport (SEA)

SEA was selected for investigation due, in part, due to its extensive noise monitor network which consists of 24 monitors with the furthest monitor located approximately 14 nmi from the airport. Noise monitors located within 6 nmi from the airport were included in the analysis. The analysis focused on three years of Boeing 737-700, Boeing 737-800, and Airbus A320 departure and arrival noise data collected from November 2021 to September 2024. Fig. 1 depicts representative flight tracks for departures and arrivals at SEA along with the noise monitor network.

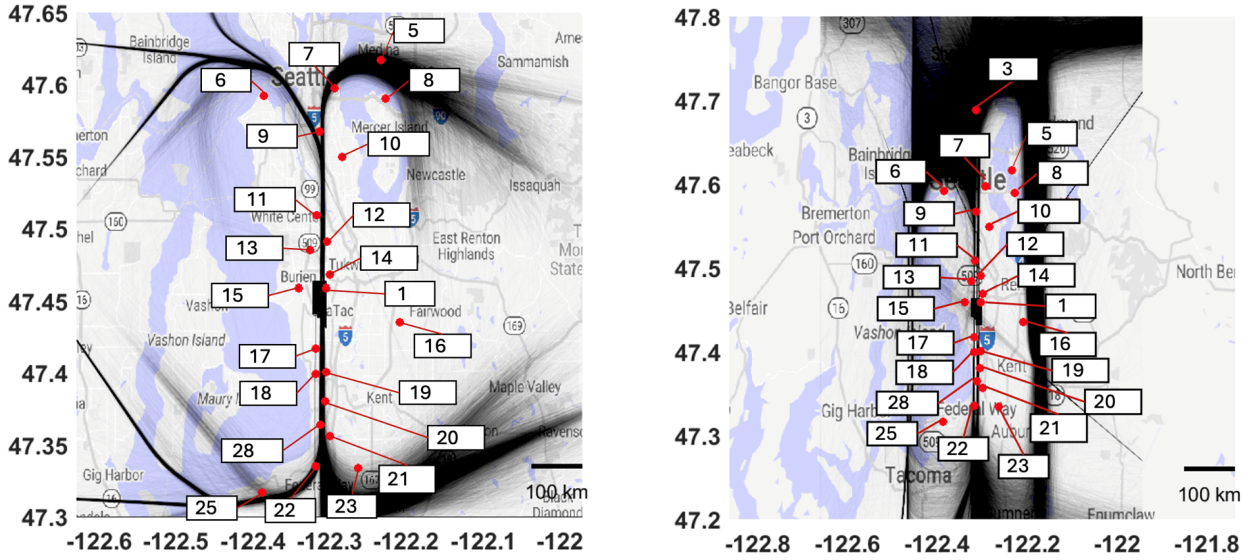

(a) Departures **(b) Arrivals**

Fig. 1 Three years of Boeing 737-800 surveillance flight tracks and noise monitor network locations, indicated in red, at SEA.

As shown in Fig. 1, SEA operations include departures and arrivals in the north and south. Due to its substantially larger dataset, southbound departures and northbound arrivals are included in this analysis of Boeing 737-700, Boeing 737-800, and Airbus A320 aircraft types. These aircraft types were selected as they represent the most commonly flown aircraft types at SEA. A summary of the SEA flights included in this analysis is shown in Table 1.

Table 1 Total count of flights at SEA used for analysis

	Boeing 737-700	**Boeing 737-800**	**Airbus A320**
Southbound Departures	19,092	69,216	12,600
Northbound Arrivals	8,406	38,763	7,271

The reported noise parameter in the monitor systems is the Sound Exposure Level (SEL) and an example distribution of observed SELs for 3 years of Boeing 737-800 southbound departures at a single representative monitor (SEA 20) located at 4.1 nmi along the departure track is shown in Fig.2. A variance of approximately 10 dB can be observed in the distribution.

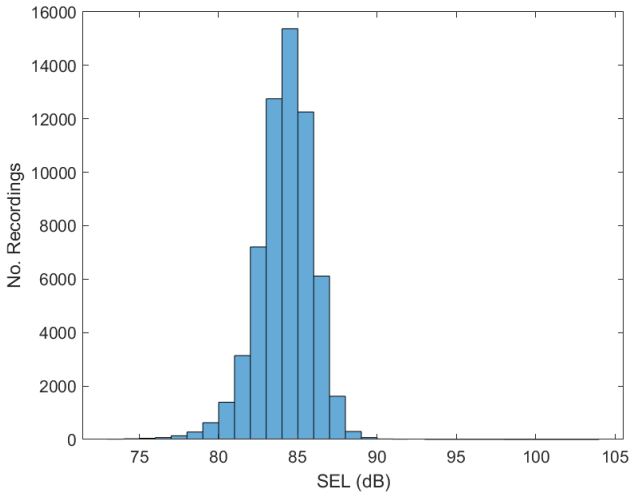

Fig. 2 Departure noise distribution for three years of Boeing 737-800 data measured by SEA 20 monitor.

2. John Wayne Airport (SNA)

The second case study airport, SNA, has a more compact noise monitor network focused on close-in noise-sensitive communities. SNA has implemented strict noise limits and severe penalties for exceeding noise thresholds in their monitoring system, resulting in airlines using aggressive noise abatement procedures on departure, particularly those to the south [19, 20]. Specifically, in order to qualify for a scheduled operation at John Wayne, a commercial airline must prove that they can operate under the Class A departure noise limits for each southbound monitor. The number of flights for each airline operating at the at the Class A noise level is limited. A higher number of flights are allowed for aircraft that can operate below a quieter Class E noise level. The Class A and Class E noise limits for the SNA southbound monitors obtained from reference [21] are shown in Table 2. If an airline's operation is approved, they them must maintain below these limits at all times or risk having the operational permission revoked [22].

Table 2 Noise Limits in single event SEL (dB) at each noise monitoring station (diagrammed in Fig. 3) for commercial airline operational classes at SNA [21]

Noise Monitor	1	2	3	4	5	6	7
Class A	102.5	101.8	101.1	94.8	95.3	96.8	93.7
Class E	94.1	93.5	90.3	86.6	87.2	87.2	86.6

The SNA noise monitor data selected for analysis includes three years of departure data taken from January 2022 to

December 2024. To allow comparison with the SEA observations the same aircraft types, Boeing 737-700, Boeing 737-800 and Airbus A320 aircraft types were assessed. Representative flight tracks at SNA and the noise monitor network are shown in Fig. 3. The SNA network consists of 10 monitors, with the furthest monitors located approximately 5 nmi to the north and 3 nmi to the south of the airport.

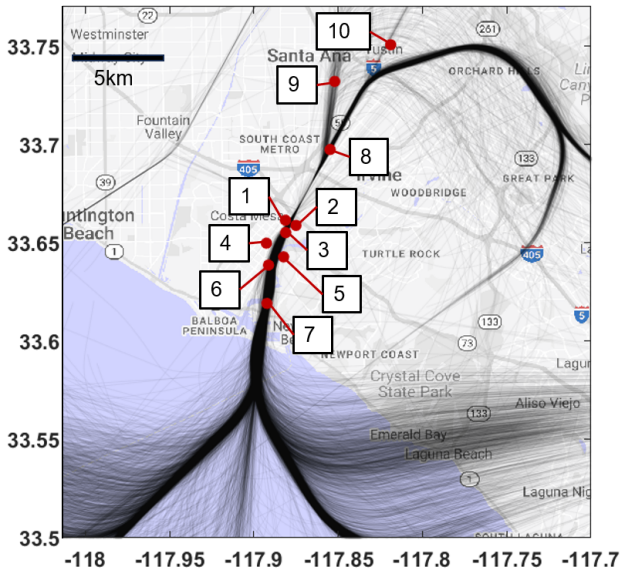

Fig. 3 Three years of Boeing 737-800 departure surveillance flight tracks and noise monitor network locations, indicated in red, at SNA

The focus of the noise restrictions on commercial aircraft at SNA are on departures to the south, which overfly sensitive communities on the coast. As a consequence, the southern monitors, SNA 1 – SNA 7, and southbound departures were selected for analysis of Boeing 737-700, Boeing 737-800, and Airbus A320 aircraft. A summary of the SNA flights included in the analysis is shown in Table 3.

Table 3 Total Count of Flights at SNA Used for Analysis

	Boeing 737-700	**Boeing 737-800**	**Airbus A320**
Southbound Departures	38,600	22,786	6,141

B. Associating Operations with Noise Data

Each noise monitor recording is correlated to a specific flight event, along with associated observed and estimated aircraft states along the trajectory. Observed states available directly from the ADS-B Opensky surveillance data [23]

include aircraft type, altitude, position, groudspeed, flight path angle, and Airline. In addition, weather factors such as wind speed and direction as well as atmospheric pressure and density were determined from the National Oceanic and Atmospheric Administration (NOAA) Rapid Refresh weather model [24] extrapolated to the time and location of the operation. The framework used to relate the aircraft surveillance, weather, and noise datasets to obtain the noise-influencing factors is shown in Fig. 4.

Derived factors related to the aircraft flight profile that are assumed to impact noise levels include thrust, weight, configuration (i.e., landing gear and high lift device position), true airspeed, and orientation. True airspeed is determined by correcting the observed ground speed with the wind components obtained from NOAA weather data. Indicated airspeed is corrected from true airspeed using pressure and density and is used to interpret the high lift device position.

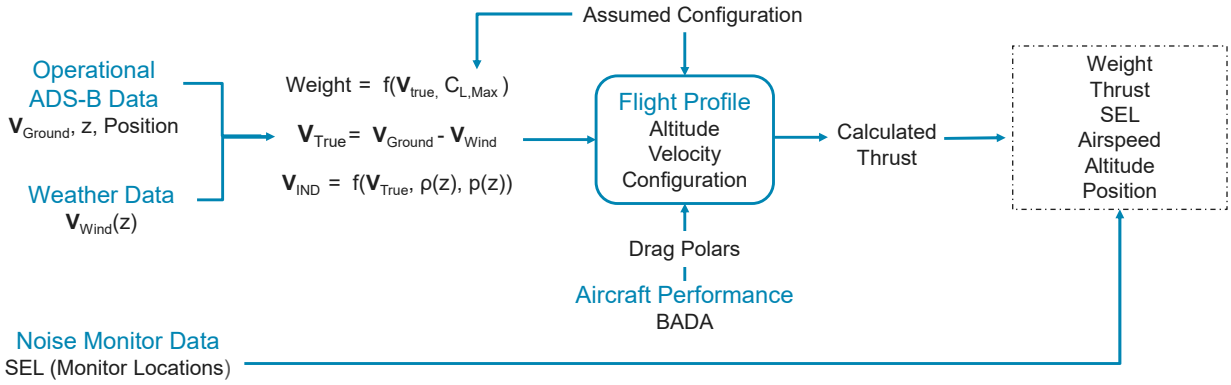

Fig. 4 Framework used to determine aircraft performance from weather and surveillance data, derived from references. [1, 2]

Airline reported takeoff weights were used for SNA but were not available for SEA. Aircraft takeoff and landing weights were therefore inferred for SEA flights from ADS-B observations of the stabilized airspeed segments during initial climb and final approach, using a method described in [25]. These speeds, visualized in Fig. 5, are normally flown at standard speeds based on the aircraft's stall speed, which varies with the weight of the aircraft. For departures, aircraft climb at approximately the takeoff safety speed, denoted V_2, plus an operational margin, ΔV_2. For arrivals, aircraft maintain the reference landing speed, V_{REF}, plus a margin ΔV_{REF}. These speeds are defined in aircraft operating manuals and certification standards to provide a safe buffer above the minimum speed at which the aircraft can sustain lift with the selected flap setting.

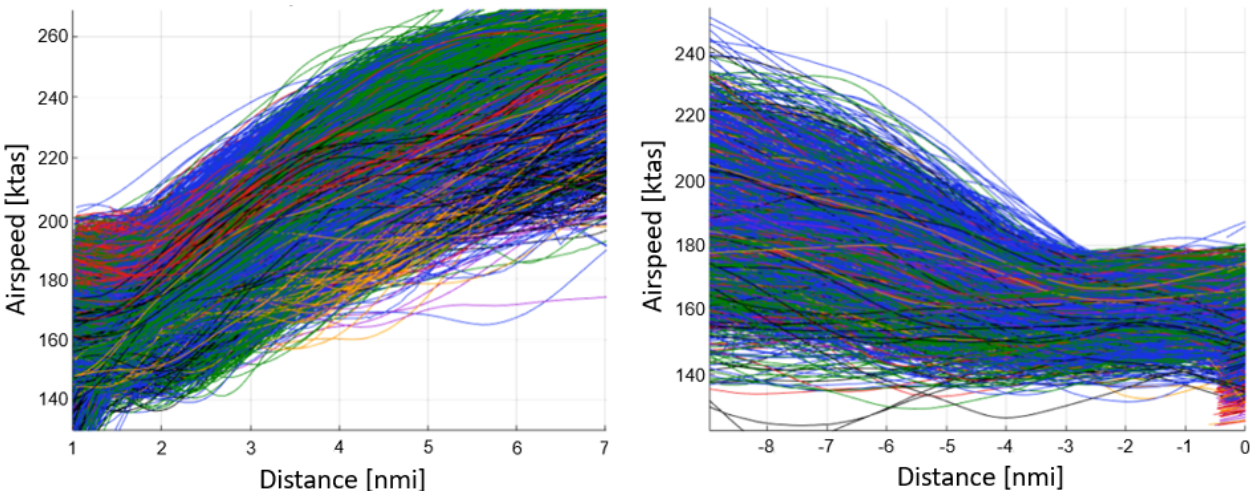

(a) Take-off speed profiles showing a stable speed segment shortly after take-off.

(b) Arrival speed profiles showing a stable speed segment shortly before landing.

Fig. 5 Typical Boeing 737-800 speed profiles at SEA during take-off and arrival (retrieved from surveillance data). Line colors represent different airlines.

Both V_2 and V_{REF} are defined as fixed multiples of the stall speed V_{stall} for the given flap configuration (e.g., $V_{\text{REF}} \approx 1.23\,V_{\text{stall}}$ for the Boeing 737 family). The stall speed depends on the aircraft weight, wing area, air density, and the maximum lift coefficient $C_{L,\max}$, which itself varies with flap deflection. Higher flap settings increase $C_{L,\max}$, lowering V_{stall}, so the reference speeds V_2 and V_{REF} change with both weight and configuration. Because stall speed increases with the square root of aircraft weight, heavier aircraft must fly at higher speeds to generate sufficient lift. As a result, by observing the stabilized true airspeed in fixed-flap, low-altitude segments at $C_{L,\max}$ values from BADA [26] and manufacturer data, the aircraft weight can be estimated. The following weight estimation method is further described in [25].

Finally, thrust was computed from a force-balance model using BADA drag polars, the inferred weight, flight path angle, and true airspeed. The full flight trajectory, including altitude, thrust, and speed evolution, is then related to observed noise at multiple monitor locations.

C. Airline-Based Analysis Approach

This section presents the analysis method used to observe operational differences between airlines. Using the procedure outlined in Sec. III.B, airspeed, altitude, and thrust profiles were created for each flight and matched with noise monitor observations. As previously noted, initial application of the behavioral clustering outlined in [7, 17],

revealed that clustering of behaviors was closely linked to airline operations. In this analysis, airlines were grouped from the airline identification in the ADS-B data to directly observe procedural differences between airlines.

An example of this grouping is shown in Fig. 6 for 3 years of Boeing 737-800 departures at SEA. Fig. 6a includes all noise observations, where individual flights are represented by lines colored according to their respective airlines (AL01 to AL08), connecting the associated noise observation at their approximate location along the departure trajectory, measured from the departure end of the runway. This raw data visualization indicates variability in observed noise levels both between and within airlines.

To better analyze the similarities and differences across airlines and the noise observations, flights were grouped by airline, as shown in 6b. The average noise profile is visualized as a solid line, with the standard deviation of the noise profile represented by the shaded region. For reference, vertical dashed lines have been placed at the location of the noise monitors. A similar process was applied to the airspeed, altitude, and thrust profiles. Flight profiles begin once valid ADS-B data is available around 0.5 nmi and continue to 6.5 nmi from the runway end. By grouping airlines, a comparative analysis of average airline behaviors for full flight trajectories can be performed.

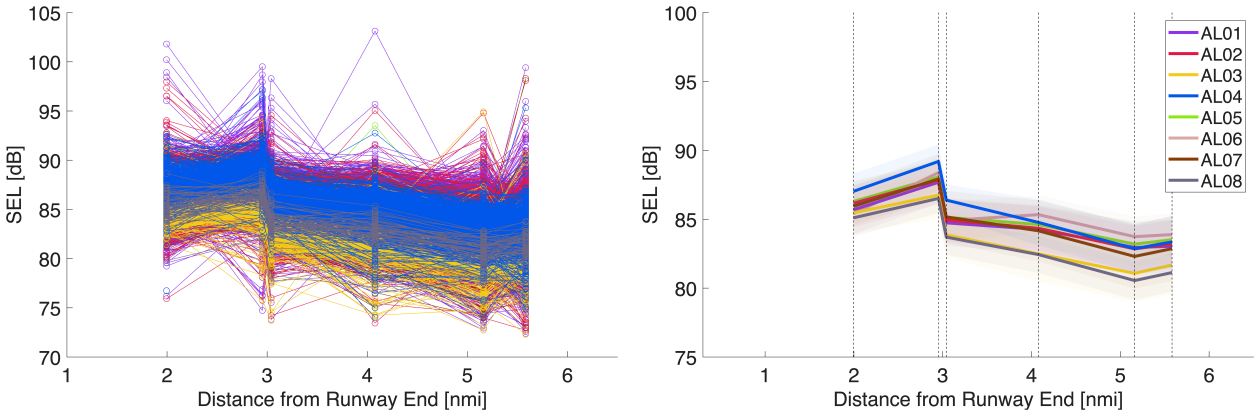

(a) Raw SEL profiles by airline

(b) Average SEL profiles by airline

Fig. 6 SEL profiles for 3 years of Boeing 737-800 SEA departures. Bold lines in (b) represent averages, and shaded areas represent region within one standard deviation. Note that vertical axes of the two figures have different scales.

As observed in Fig. 6, it is notable that there is a consistent difference observed in noise levels at monitors SEA 18 and SEA 19, located at similar distances (approximately 3 nmi) from the runway end. This was observed for departures of all aircraft types, with the monitor at 2.9 nmi (SEA 19) recording approximately 2.5dB higher SEL levels than the monitor at 3.1 (SEA 18). The differences are partly attributable to the differences in lateral distance from the average

ground track, with the average flight passing approximately 0.38 nmi east of monitor SEA 18 while only approximately 0.21 nmi west of monitor SEA 19. Additional considerations include instrument calibration and local terrain effects, which could cause local amplification or blocking of noise from the direction of the departure trajectories.

IV. Assessment of Factors Contributing to Departure and Arrival Noise

In the following subsections, comparative analysis by airline is presented for departures and arrivals from SEA and departures from SNA.

A. Southbound Departures at SEA

As can be seen in the noise profiles for Boeing 737-800 departures in Fig. 7, AL04 (blue), AL05 (green), and AL06 (peach) are loudest at all monitors, while AL03 (yellow) and AL08 (grey) are the quietest on average. The noise ordering generally correlates with the relative weights and average thrust levels of each airline, with increasing weight and thrust level indicating higher noise.

Another notable feature is the significantly higher average thrust for AL04 (blue) throughout the entire departure. This high thrust not only correlates with higher noise at all monitors but also allows AL04 (blue) to fly an operational procedure which prioritizes steeper climb beyond 3 nmi, even while maintaining relatively high airspeed. This strategy results in noise observations that are 1 – 2 dB higher than other airlines on average when within 3 nmi of the airport, but that are also 0.5 – 1 dB quieter than the loudest airline beyond 3 nmi due to the higher altitude.

This strategy contrasts with both AL05 (green) and AL06 (peach) which both fly aircraft with high weights but also lower initial thrust levels, perhaps using de-rated thrust, and apply an additional thrust cutback between 2 – 3 nmi. The thrust cutback and lower thrust results in lower noise compared to AL04 (blue) near the airport, but results in a lower climb rate; the noise diminishes more slowly beyond 3 nmi resulting in the highest noise levels outside of 4 nmi due to the lower altitudes. AL03 (yellow) and AL08 (grey) have the lowest weight and have the lowest noise levels at all monitors and fly quite similar departure profiles with a power cutback at 1.5 and 3 nmi and a intermediate speed climb of approximately 210 kts between between 3.5 – 5 nmi.

AL01 (purple), AL02 (red), and AL07 (brown) each have a noise profiles which fall in the middle of the airline distribution. Each exhibit a constant acceleration throughout the departure with AL01 (purple) and AL02 (red) applying a thrust cutback between 1 and 2 nmi and climb shallower beyond 3 nmi, while AL07 (brown) uses less cutback and

climbs at a consistent rate on average through the entire profile. By prioritizing climb rate and altitude, AL07 (brown) has lower noise levels at the monitors outside of 4 nmi than AL01 (purple) and AL02 (red).

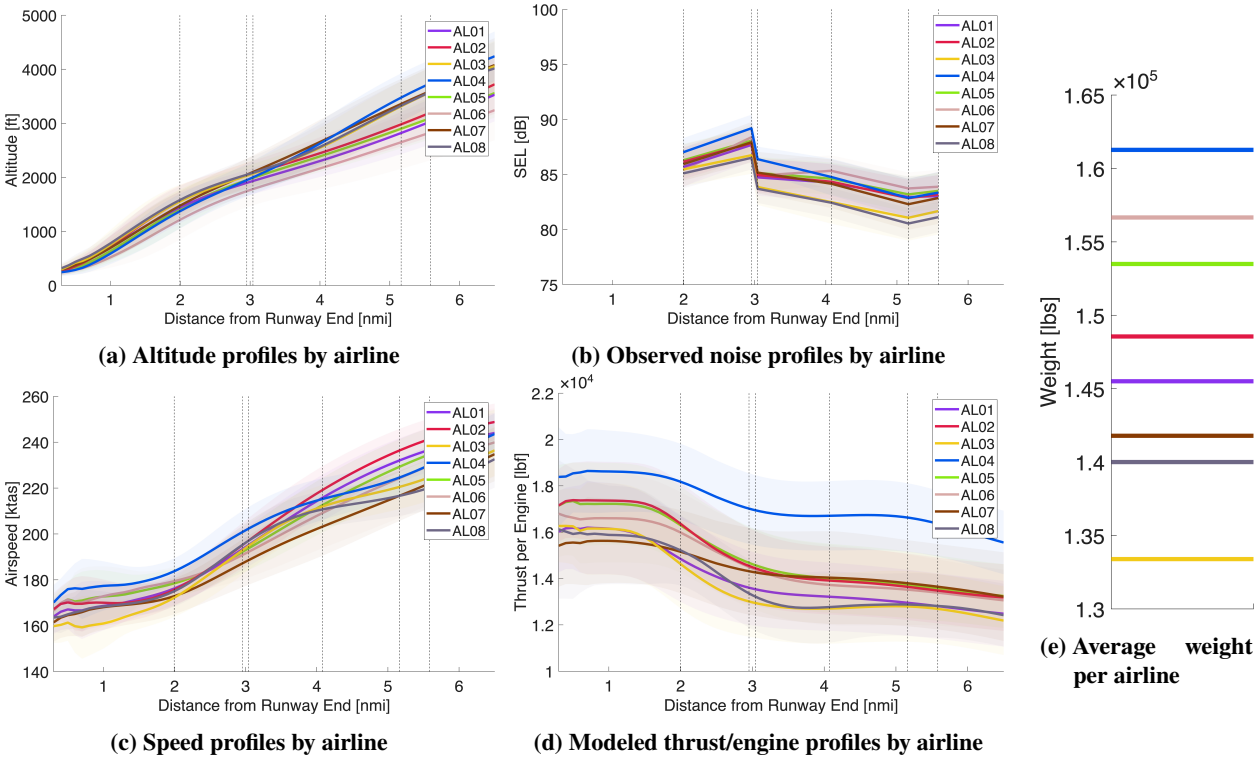

(a) Altitude profiles by airline

(b) Observed noise profiles by airline

(c) Speed profiles by airline

(d) Modeled thrust/engine profiles by airline

(e) Average weight per airline

Fig. 7 Boeing 737-800 departure profiles at SEA for different airlines. Bold lines represent averages, and shaded areas represent region within one standard deviation.

For the Boeing 737-700 aircraft shown in Fig. 8, many similar trends emerge. For example, AL04 (blue) again has the highest weight, and high thrust with no apparent thrust cutback resulting in the highest noise levels at all monitors.

AL01 (purple) and AL03 (yellow) have noise observations that are within 0.5 dB of each other at monitors within 3 nmi of the airport, but AL01 (purple) has observations that are approximately 2 dB higher than AL03 (yellow) beyond 3 nmi. Both airlines have similar weights and thrust profiles with a gentle thrust cutback on average. However, as observed with the Boeing 737-800 departures, AL01 (purple) uses this thrust to accelerate at a consistent rate from 3 – 5 nmi, while AL03 (yellow) accelerates more slowly in order to gain altitude more quickly, which leads to a noise reduction for AL03 (yellow) beyond 3 nmi.

AL08 (grey) is louder than AL01 (purple) and AL03 (yellow) at monitors within 3 nmi of the airport but becomes quieter than AL01 (purple) beyond 3 nmi. AL08 (grey) does not exhibit a thrust cutback and maintains a relatively slow second segment climb speed of 200 kts resulting in higher altitudes and lower noise than AL01 (purple) outside of 4 nmi.

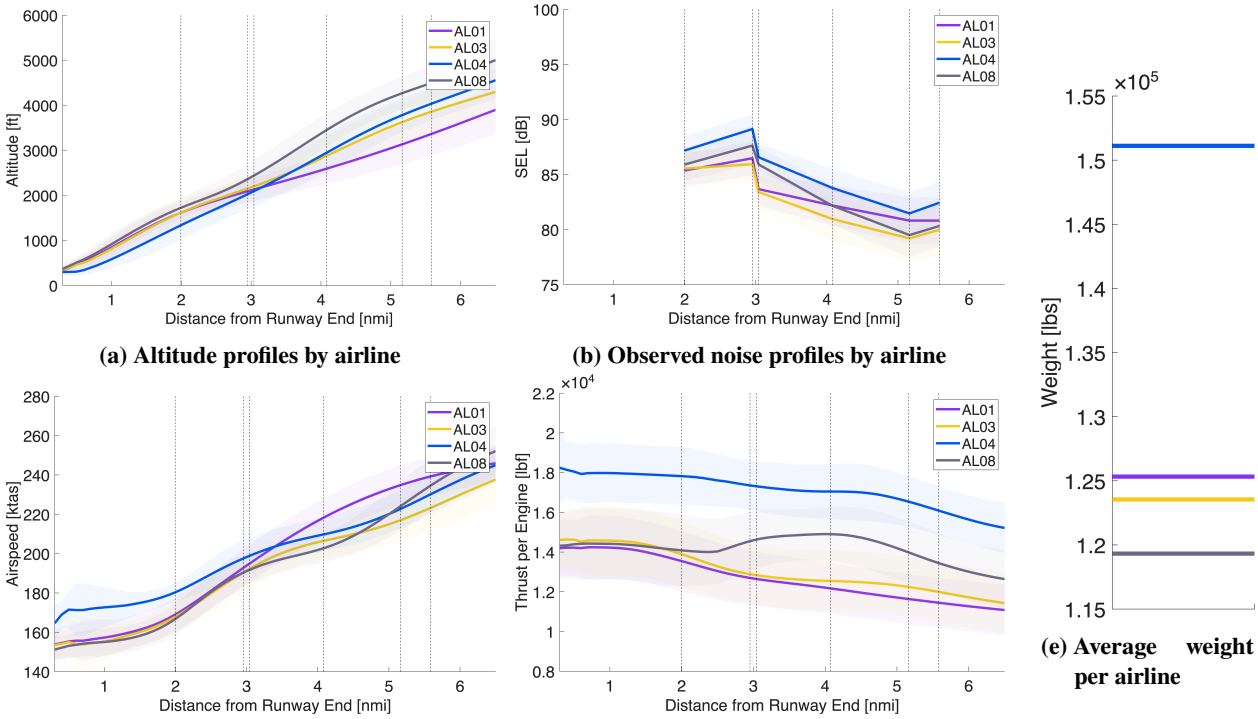

(a) Altitude profiles by airline

(b) Observed noise profiles by airline

(c) Speed profiles by airline

(d) Modeled thrust/engine profiles by airline

(e) Average weight per airline

Fig. 8 Boeing 737-700 departure profiles at SEA. Bold lines represent averages, and shaded areas represent region within one standard deviation.

Considering the Airbus A320 departures shown in Fig. 9, similar profile structure can be seen for all airlines, with differences primarily being driven by differences in weight with higher thrust and lower altitudes for the higher weight airlines. AL05 (light green) is an exception, as it has high average weight and uses higher thrust than all other airlines, yet has low noise levels. The average noise levels for most of the airlines are within 1.5 dB with the exception of AL02 (red) which is approximately 4 dB higher than the others at all monitors. While AL02 (red) has high weights the noise difference is greater than would expected due to operational reasons and it is thought to be due to airframe differences. The original Airbus A320 design had a known tonal noise source from a fuel vent port at approach and departure speeds [27] which can be suppressed with a vortex generator. Most airlines have incorporated this modification however AL02 (red) has reportedly not added the vortex generator modification to its fleet.

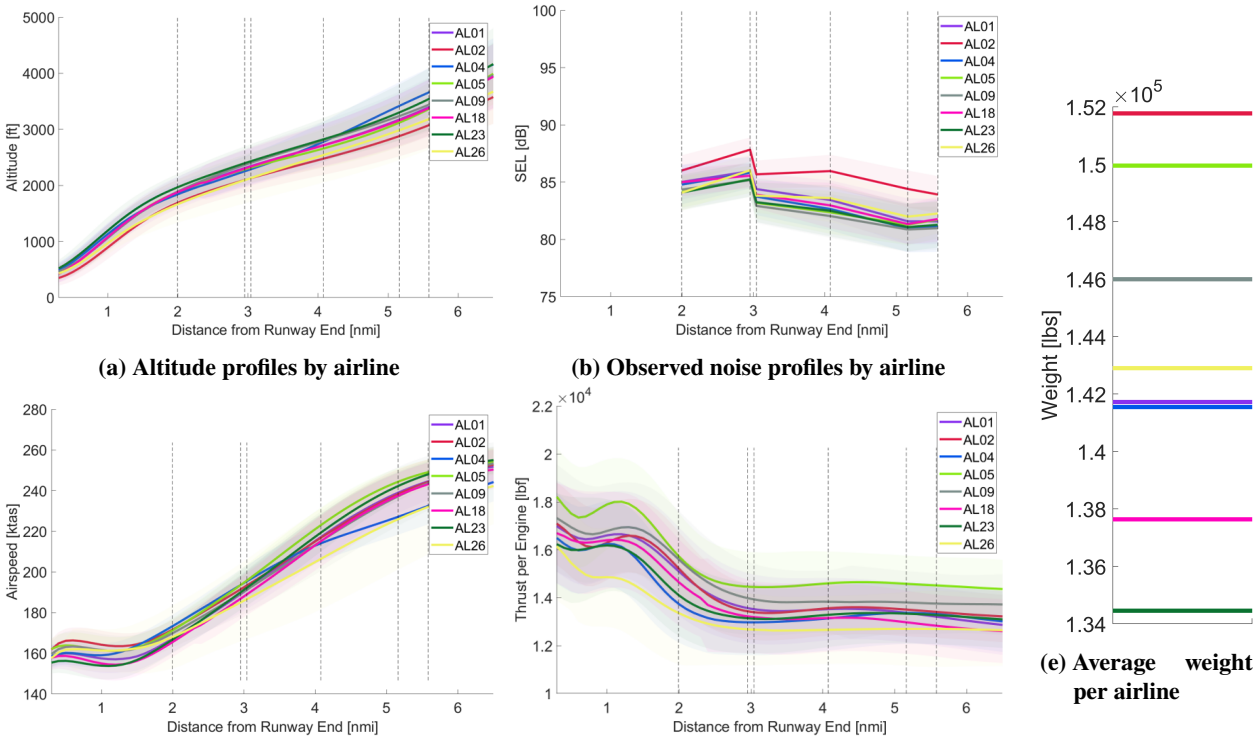

(a) Altitude profiles by airline

(b) Observed noise profiles by airline

(e) Average weight per airline

(c) Speed profiles by airline

(d) Modeled thrust/engine profiles by airline

Fig. 9 Airbus A320 departure profiles at SEA. Bold lines represent averages, and shaded areas represent region within one standard deviation.

B. Northbound Arrivals at SEA

As can be seen in the arrival profiles for Boeing 737-800 departures shown in Fig. 10, there is very little difference in altitude profile between airlines indicating close tracking of the instrument landing system glideslope. The approach speeds generally correlate with weight for the entire approach and weight correlates with average noise levels near the airport within 2 nmi of the airport. For example, AL08 (grey) which is heaviest and fastest on average also has the highest noise levels. AL02 (red) is a slight exception as it flies relatively light aircraft with slower airspeeds but exhibits relatively higher noise observations at monitors inside of 4 nmi. AL02 (red) also exhibits higher thrust at these locations compared to the other lower-airspeed airlines.

A notable outlier in the noise profiles is the high noise levels observed by AL08 (grey) at the monitor approximately 4 nmi from the airport, where it is approximately 3 dB louder than any other airline. AL08 (grey) has the highest average weight and a high average speed of 168 knots at this monitor. It is likely that the higher noise is due to later deployment of flaps and increased airframe noise due to the higher speed.

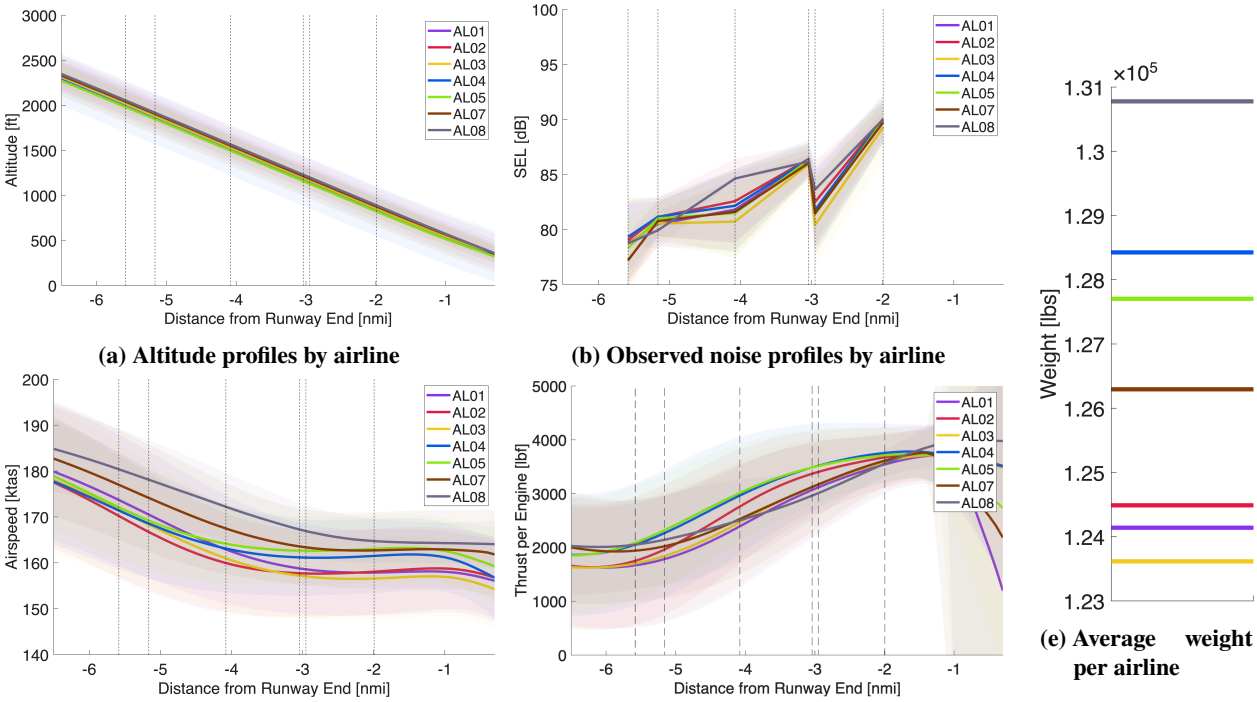

(a) Altitude profiles by airline

(b) Observed noise profiles by airline

(c) Speed profiles by airline

(d) Modeled thrust profiles by airline

(e) Average weight per airline

Fig. 10 Boeing 737-800 arrival profiles at SEA. Bold lines represent averages, and shaded areas represent region within one standard deviation.

The Boeing 737-700 profiles shown in Fig. 11 indicate many of the same trends. Again, weight correlates with airspeed which correlates with noise. Also, AL08 (grey) again has the highest weight and exhibits higher noise levels by approximately 4 dB at the 4 nmi monitor where it is flying approximately 165 knots, which is faster than any other airline.

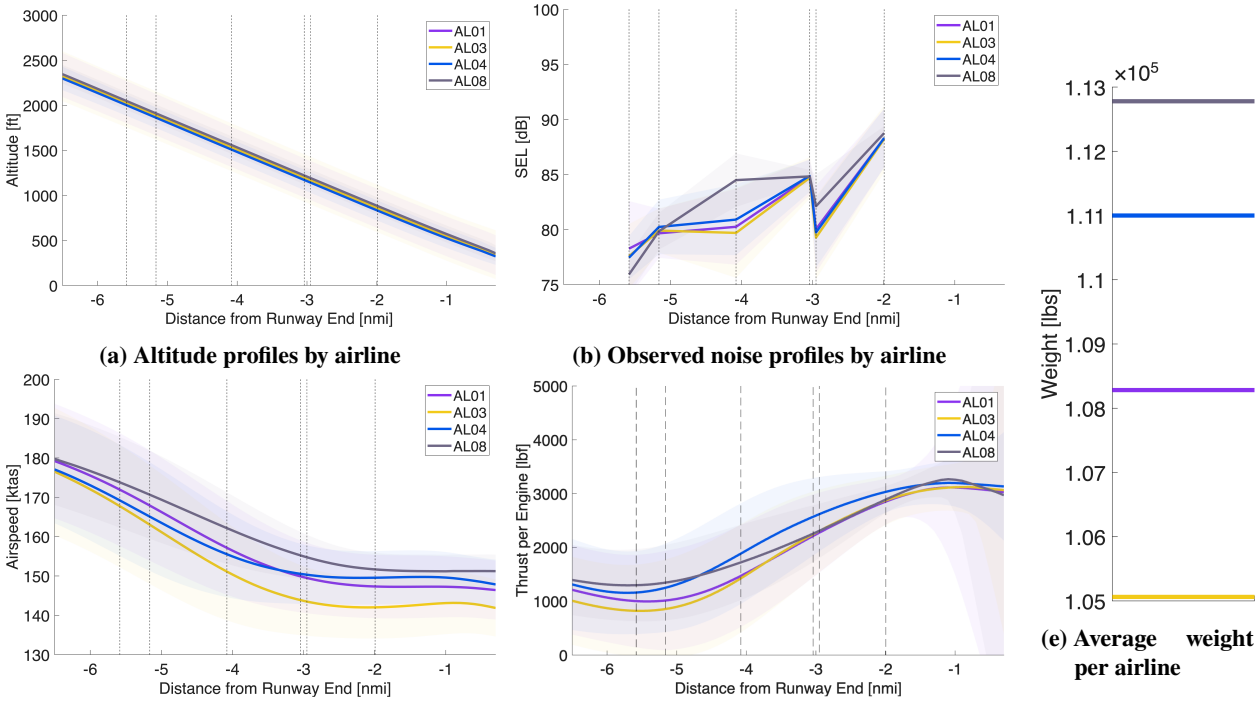

(a) Altitude profiles by airline

(b) Observed noise profiles by airline

(c) Speed profiles by airline

(d) Modeled thrust/engine profiles by airline

(e) Average weight per airline

Fig. 11 Boeing 737-700 arrival profiles at SEA. Bold lines represent averages, and shaded areas represent region within one standard deviation.

The Airbus A320 arrival profiles shown in Fig. 12, show slightly more variation in noise than the Boeing variants. For example, AL02 (red) and AL18 (magenta) are loudest at all monitors despite having lower weight. This may be due to the fuel vent noise source discussed above regarding the Airbus A320 departures. Outside of 3 nmi there is significant variability in observed noise that does not clearly correlate with flight condition likely due to changes in flap configuration which occur during this decelerating phase of flight.

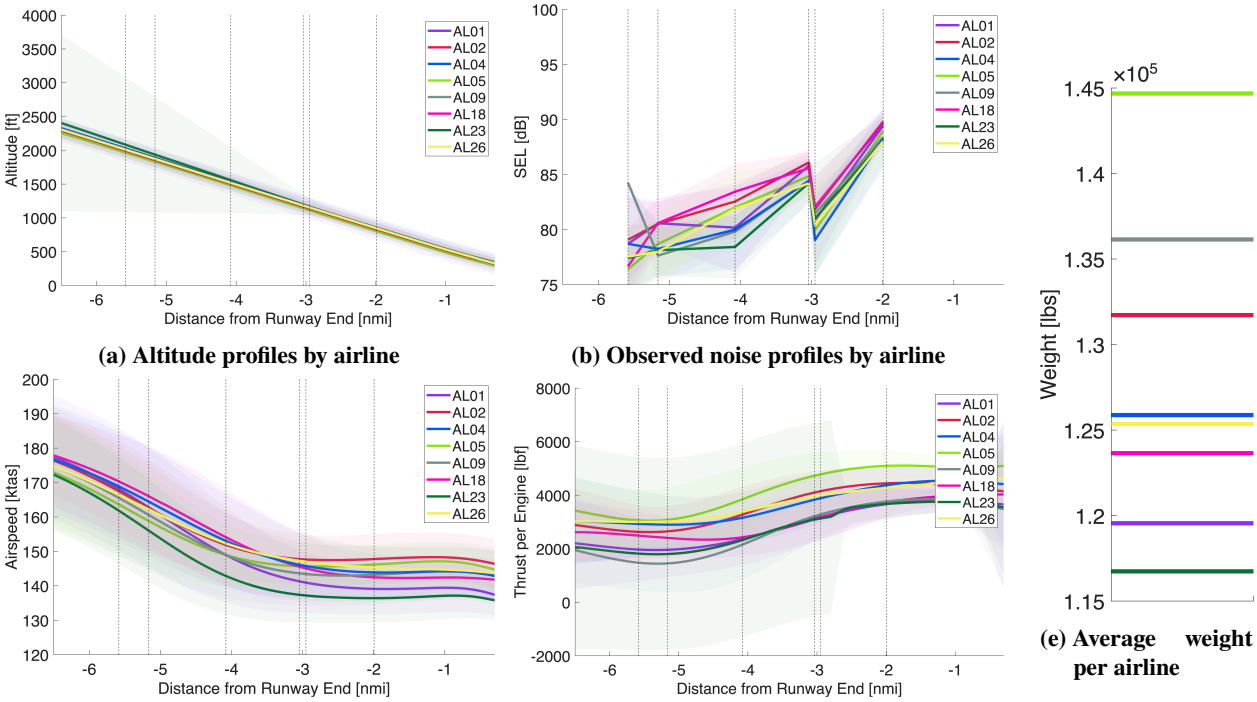

(a) Altitude profiles by airline

(b) Observed noise profiles by airline

(c) Speed profiles by airline

(d) Modeled thrust/engine profiles by airline

(e) Average weight per airline

Fig. 12 Airbus A320 arrival profiles at SEA. Bold lines represent averages, and shaded areas represent region within one standard deviation.

C. Southbound Departures at SNA

The departure profiles for Boeing 737-800 departures from SNA are shown in Fig. 13 which also includes the restrictive Class E noise limits at each of the monitors. AL03 (yellow) has significantly lower noise levels at all monitors and is close to or under the Class E noise limits. AL03 (yellow) achieves these low noise levels through low weight which allows lower initial thrust and an aggressive thrust cutback which starts inside of 1 nmi and continues until past the monitors. AL03 (yellow) also holds speed at 165 knots until past the monitors. AL02 (red) also flies at low weight with a similar, but late,r aggressive thrust cutback which starts outside of 1 nmi and a 165 knot constant speed climb but does not meet the Class E noise limits likely due to the fuel vent noise source discussed above.

All other airlines also exceed the Class E limits and the observed noise levels generally correlate with weight however there is a significant difference in flight profiles. The airlines with the highest weight, AL04 (blue) and AL05 (green), have an early power cutback between 1 and 1.5 and climb at a low airspeed of approximately 165 knots until past the monitors at 3 nmi. AL01 (purple) has a lower weight and does not have as significant a thrust cutback but starts accelerating during the departure and has a lower climb rate and lower altitude.

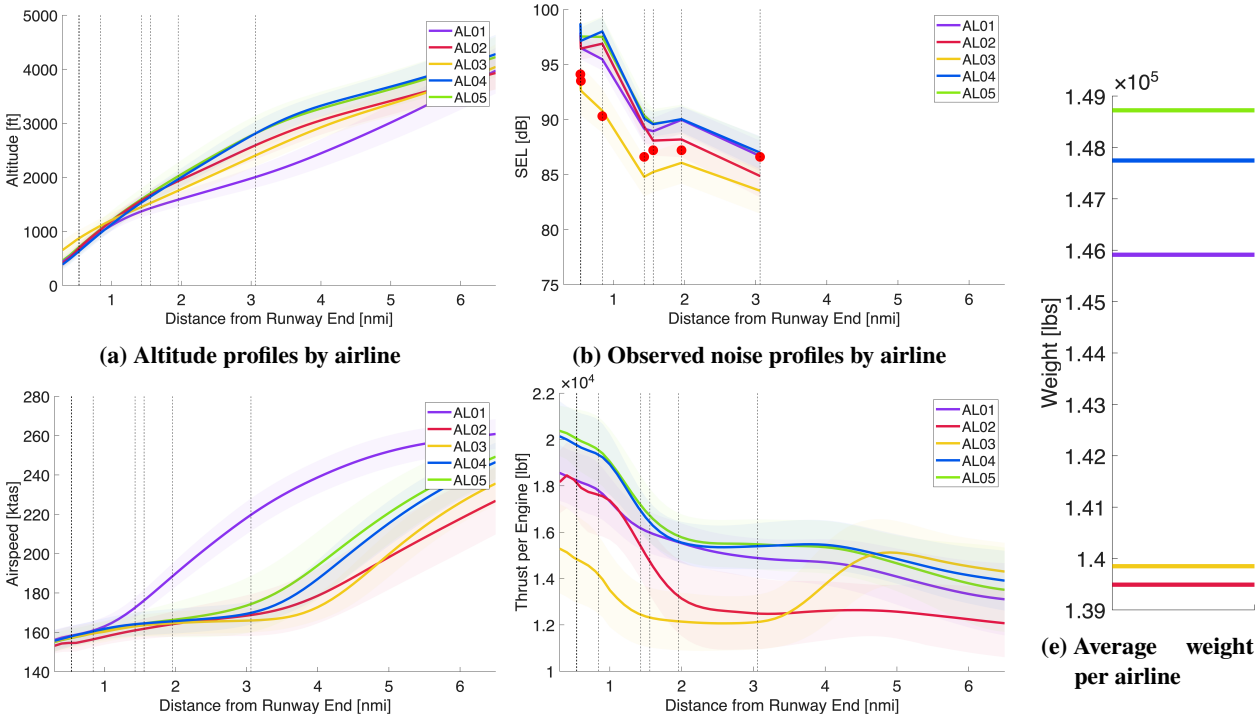

(a) Altitude profiles by airline

(b) Observed noise profiles by airline

(c) Speed profiles by airline

(d) Modeled thrust/engine profiles by airline

(e) Average weight per airline

Fig. 13 Boeing 737-800 departure profiles at SNA. Bold lines represent averages, shaded areas represent region within one standard deviation, red dots represent Class E operation noise limits.

The departure profile for the Boeing 737-700s are shown in Fig. 14. AL03 (yellow) again has significantly lower noise levels at all monitors and is under the Class E noise limits. AL03 (yellow) achieves these low noise levels through low weight which allows lower initial thrust and an aggressive thrust cutback which starts inside of 1 nmi and continues until past the monitors. AL03 (yellow) also holds speed at 150 knots until past the monitors. The other airlines all exceed the Class E limits but exhibit a variety of procedures. AL02 (blue) has the highest weight with relatively high thrust and and holds a constant airspeed of approximately 160 knots until past the monitors. AL08 (grey) accelerates to an intermediate climb speed of approximately 210 knots until past the monitors while AL01 (purple) has a continuous acceleration throughout the departure.

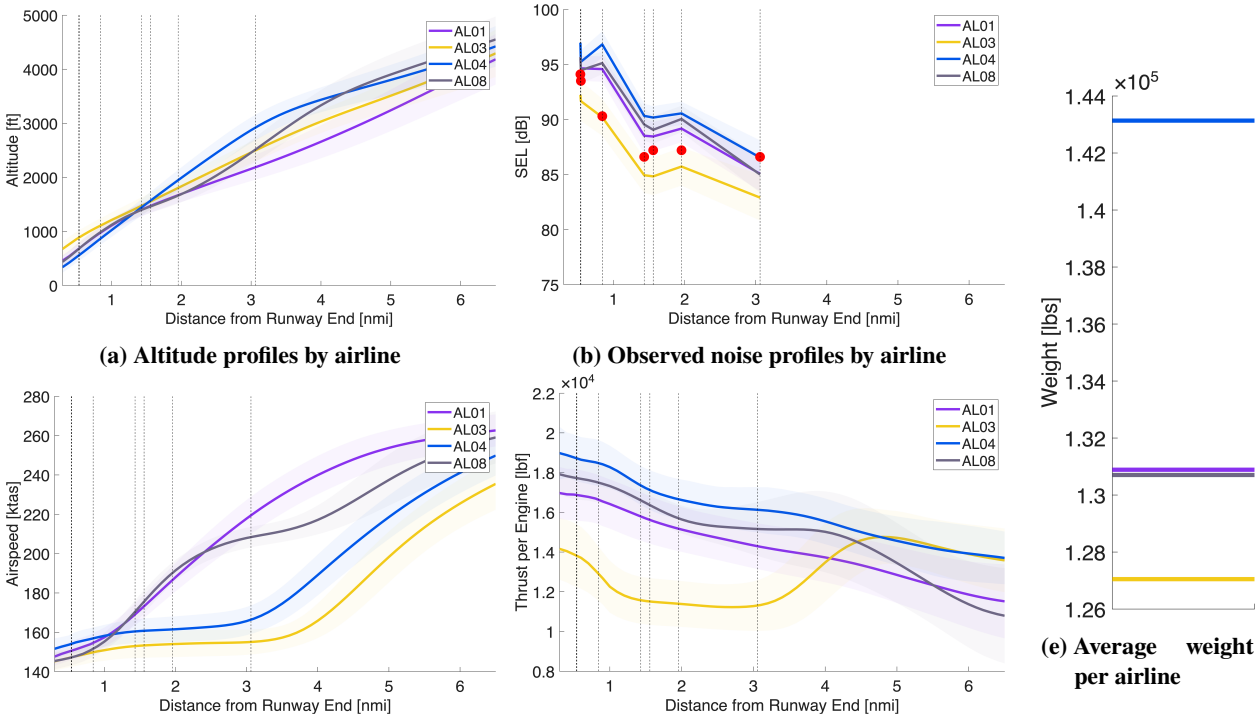

(a) Altitude profiles by airline

(b) Observed noise profiles by airline

(c) Speed profiles by airline

(d) Modeled thrust/engine profiles by airline

(e) Average weight per airline

Fig. 14 Boeing 737-700 departure profiles at SNA. Bold lines represent averages, shaded areas represent region within one standard deviation, red dots represent Class E operation noise limits.

The departure profiles for the Airbus A320s are shown in Fig. 15. With the exception of AL23 (green) which operates at very low weight, all airlines exceed the Class E noise limits inside of 1.5 nmi but are below the limits outside of 1.5 nmi. The noise levels correlate with weight and thrust inside of 1.5 nmi. Most airlines have a thrust cutback at 1 nmi and hold constant speed until past the monitors at 3 nmi except AL02 (red) and AL18 (magenta) which accelerate during the climb with lower climb rates and higher noise levels.

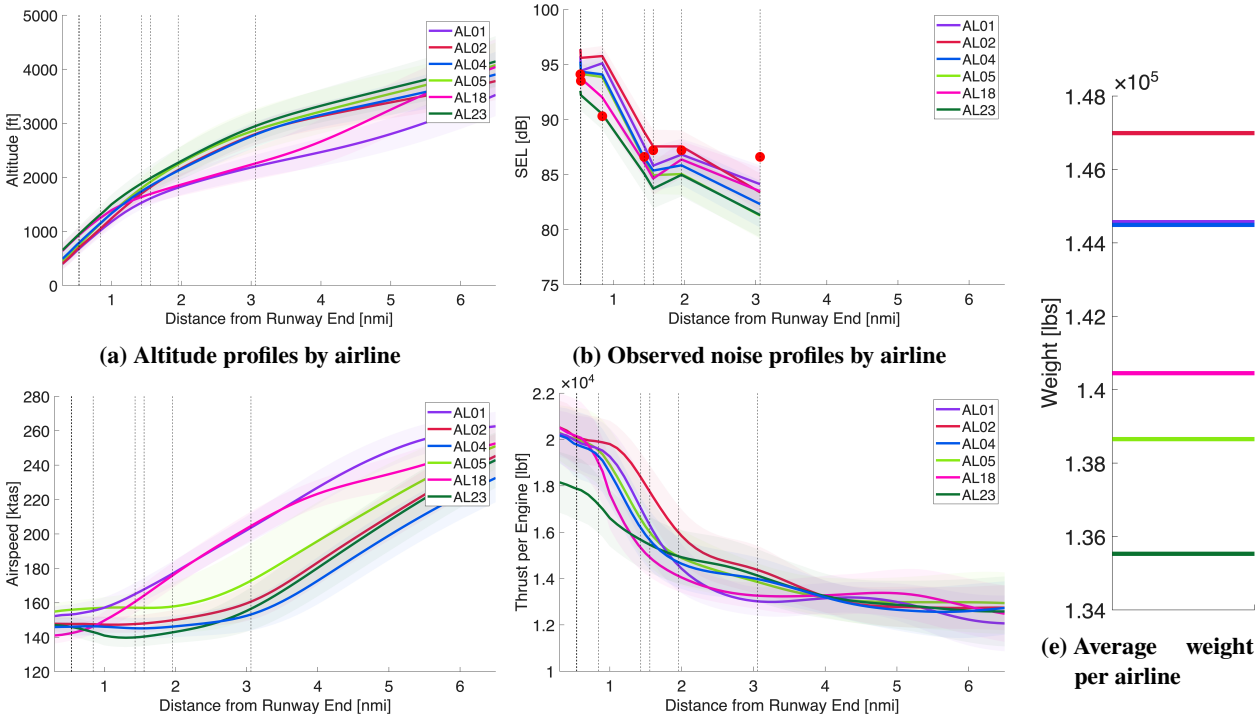

(a) Altitude profiles by airline

(b) Observed noise profiles by airline

(c) Speed profiles by airline

(d) Modeled thrust/engine profiles by airline

(e) Average weight per airline

Fig. 15 Airbus A320 departure profiles at SNA. Bold lines represent averages, shaded areas represent region within one standard deviation, red dots represent Class E operation noise limits.

V. Conclusion

The comparative analysis of airline grouped trajectories of Boeing 737-800, Boeing 737-700, and Airbus A320 departures and arrivals at Seattle-Tacoma International Airport (SEA) and departures at John Wayne International Airport (SNA) identified operational factors and procedural differences between airlines which influenced observed noise levels.

For departures, aircraft weight strongly influenced observed noise. Higher weight aircraft generally operated at higher thrust levels and had lower climb rates resulting in higher noise levels. Procedural differences in thrust management were also observed. Several airlines such as AL04 (blue) and AL08 (grey) at SEA were observed to operate at high thrust levels on average with limited thrust reductions on initial climb resulting in higher noise levels particularly at monitors closer to the airport. This may be due to conservative thrust de-rate procedures. Other airlines operated at lower thrust levels with thrust reductions on initial climb which reduced noise close to the airport. The thrust reductions were earlier and more aggressive at SNA which has noise restrictions at monitors close to the airport. The thrust reductions were most extreme for the lightweight AL03 Boeing 737-700 and Boeing 737-800 departures

which result in lower noise levels close to or below more restrictive Class E noise limits at SNA.

The airline-averaged flight profiles at SEA and SNA also revealed trends in the observed noise. On departure, heavier aircraft typically require more thrust and thus emit more noise for all aircraft types at both airports. Within 3 nmi of the airport, reduced thrust correlated with reduced noise. Operational strategies which impact climb rate and their relation to noise are apparent. With steeper climbs achieved through higher thrust levels or slower climb speeds, the higher altitudes result in lower noise outside of approximately 3 nmi, although the higher thrust levels may result in higher noise at closer monitors.

The impact of aircraft source noise was also apparent with the Airbus A320, which generally exhibited lower noise levels at similar monitor locations than the Boeing 737-800 and Boeing 737-700 departures. This is not true for AL02's (red) Airbus A320 aircraft which were consistently louder than other airlines flying this aircraft, likely due to a fuel vent tonal noise source.

For arrivals, thrust and weight are more weakly correlated with noise differences correlating more closely with airspeed behaviors, which influence aircraft configuration during deceleration through flap airspeed limits, and the strong effect of velocity on flap source noise.

Acknowledgments

This work was sponsored by the Federal Aviation Administration (FAA) under ASCENT Center of Excellence Project 44 (grant number 13-C-AJFE-MIT-050). Opinions, interpretations, conclusions, and recommendations are those of the authors and are not necessarily endorsed by the United States Government. The authors would like to acknowledge the support of Chris Dorbian and Joseph DiPardo of the FAA Office of Environment and Energy as well as the Massachusetts Port Authority and HMMH.

References

[1] Mahseredjian, A., Huynh, J., and Hansman, R. J., "Analysis of community departure noise exposure variation using airport noise monitor networks and operational ADS-B data," *INTER-NOISE and NOISE-CON Congress and Conference Proceedings*, Vol. 265, No. 4, 2023, pp. 3172–3190. https://doi.org/10.3397/IN_2022_0447.

[2] Huynh, J., Mahseredjian, A., and Hansman, R. J., "Delayed Deceleration Approach Noise Impact and Modeling Validation," *Journal of Aircraft*, Vol. 59, No. 4, 2022. https://doi.org/10.2514/1.C036631.

[3] Zorumski, W. E., "Aircraft Noise Prediction Program (ANOPP) Theoretical Manual," Tech. Rep. NASA-TM-83199, NASA, 1981.

[4] Fleming, G. G., "Aviation Environmental Design Tool (AEDT)," Tech. Rep. DOT-VNTSC-FAA-16-11, Federal Aviation Administration, Washington, DC, 2016.

[5] Giladi, R., "Real-time identification of aircraft sound events," *Transportation Research Part D: Transport and Environment*, Vol. 87, Oct. 2020, p. 102527. https://doi.org/10.1016/j.trd.2020.102527.

[6] Jäger, D., Zellmann, C., Wunderli, J. M., Scholz, M., Abdelmoula, F., and Gerber, M., "Validation of an airline pilot assistant system for low-noise approach procedures," *Transportation Research Part D: Transport and Environment*, Vol. 99, Oct. 2021, p. 103020. https://doi.org/10.1016/j.trd.2021.103020.

[7] Li, C., and Hansman, R. J., "Hierarchical Behaviors for Characterizing Trajectory Patterns in Terminal Airspace," *AIAA SCITECH 2024 Forum*, 2024. https://doi.org/10.2514/6.2024-2354.

[8] Rafanambinantsoa, V. C., Muraretu, I. D., Dimbisoa, W. G., Mahatody, T., Bãdicã, C., and Razafindrakoto, R., "Modelling aircraft noise map around an airport using machine learning," *2024 International Conference on INnovations in Intelligent SysTems and Applications (INISTA)*, IEEE, 2024, pp. 1–8. https://doi.org/10.1109/INISTA62901.2024.10683826.

[9] Toraman, S., Dursun, O. O., and Aygun, H., "Prediction of noise of commercial aircraft based on itself specifications by using machine learning methods," *Journal of Air Transport Management*, Vol. 125, May 2025, p. 102779. https://doi.org/10.1016/j.jairtraman.2025.102779.

[10] European Union Aviation Safety Agency, "Aircraft Noise and Performance (ANP) Data," www.easa.europa.eu/en/domains/environment/policy-support-and-research/aircraft-noise-and-performance-anp-data, 2025.

[11] Zhu, D., Peng, J., and Ding, C., "A Neural Network with Physical Mechanism for Predicting Airport Aviation Noise," *Aerospace*, Vol. 11, No. 9, 2024. https://doi.org/10.3390/aerospace11090747.

[12] Nakayama, T., Kouda, S., and Yokota, T., "Application of machine learning in aircraft noise monitoring: Determining disturbance sounds within aircraft noise events," *Acoustical Science and Technology*, Vol. advpub, 2024, p. e24.68. https://doi.org/10.1250/ast.e24.68.

[13] Pak, J.-w., and Kim, M.-k., "Convolutional Neural Network Approach for Aircraft Noise Detection," *2019 International Conference on Artificial Intelligence in Information and Communication (ICAIIC)*, IEEE, 2019, pp. 430–434. https://doi.org/10.1109/ICAIIC.2019.8669006.

[14] Envia, E., "Fan Noise Source Diagnostics Test - Vane Unsteady Pressure Results," *8th AIAA/CEAS Aeroacoustics Conference & Exhibit*, Breckenridge, 2002. https://doi.org/10.2514/6.2002-2430.

[15] Alonso, J. J., Alonso, Y., Shukla, A., Jackson, D., and Rindfleisch, T., "Improving Noise Predictions of the Aviation Environmental Design Tool (AEDT) Using Deep Neural Networks and Sound-level Monitor Data," *AIAA SCITECH 2023 Forum*, 2023. https://doi.org/10.2514/6.2023-0735.

[16] Feng, H., Zhou, Y., Zeng, W., and Guo, W., "A physics-based PSO-BPNN model for civil aircraft noise assessment," *Applied Acoustics*, Vol. 221, Mar 2024, p. 109992. https://doi.org/10.1016/j.apacoust.2024.109992.

[17] Li, C., "Hierarchical Behavior Models for Characterizing Trajectories within Terminal Airspace," Ph.D. thesis, Massachusetts Institute of Technology, 2024, https://hdl.handle.net/1721.1/155395.

[18] Lepe, M., Homola, M., Li, C., Lee, T., Hood, P., Huynh, J. L., and Hansman, R. J., "Multifactor Analysis of Operational Factors Contributing to Aircraft Overflight Noise Variation," *AIAA SCITECH 2025 Forum*, American Institute of Aeronautics and Astronautics, 2025. https://doi.org/10.2514/6.2025-2004.

[19] Irving, D., "Steep takeoffs land JWA on 'scariest airports' list," https://www.ocregister.com/2012/07/20/steep-takeoffs-land-jwa-on-scariest-airports-list/, 2012. Accessed: 2025–11–01.

[20] Murphy, D. W., "The impact of transport category aircraft departure profiles on community noise exposure in the vicinity of John Wayne Airport, Orange County," Vol. 84, 1988, pp. S222–S222. https://doi.org/10.1121/1.2026212.

[21] John Wayne Airport, "Noise Limits," https://www.ocair.com/about/administration/access-noise/reports-resources/noise-limits, 2025. Accessed: 2025-11-28.

[22] John Wayne Airport, "Phase 2 Commercial Airline Access Plan and Regulation," https://files.ocair.com/media/2021-02/Access-Plan_2021-01_web.pdf?VersionId=n5OrJQ1oL939ZdAsxI79Izoowxg7xpZ4, 1990. Accessed: 2025-11-28.

[23] Schafer, M., Strohmeier, M., Lenders, V., Martinovic, I., and Wilhelm, M., "Bringing up OpenSky: A large-scale ADS-B sensor network for research," *IPSN-14 Proceedings of the 13th International Symposium on Information Processing in Sensor Networks*, IEEE, 2014, pp. 83–94. https://doi.org/10.1109/IPSN.2014.6846743.

[24] Benjamin, S. G., Weygandt, S. S., Brown, J. M., Hu, M., Alexander, C. R., Smirnova, T. G., Olson, J. B., James, E. P., Dowell, D. C., Grell, G. A., Lin, H., Peckham, S. E., Smith, T. L., Moninger, W. R., Kenyon, J. S., and Manikin, G. S., "A North American Hourly Assimilation and Model Forecast Cycle: The Rapid Refresh," *Monthly Weather Review*, Vol. 144, No. 4, 2016, pp. 1669–1694. https://doi.org/10.1175/MWR-D-15-0242.1.

[25] Homola, M., Lepe, M., Trávník, M., Huynh, J. L., and Hansman, R. J., "Take-Off and Landing Weight Estimation From ADS-B Airspeed Profiles," *AIAA AVIATION FORUM AND ASCEND 2025*, Las Vegas, NV, 2025. https://doi.org/10.2514/6.2025-3309.

[26] Nuic, A., "User Manual for the Base of Aircraft Data (BADA) Revision 3.12," Tech. Rep. 12/11/22-58, Eurocontrol, 2013.

[27] Pott-Pollenske, M., Dobrzynski, W., Buchholz, H., Gehlhar, B., and Walle, F., "Validation of a Semiempirical Airframe Noise Prediction Method Through Dedicated A319 Flyover Noise Measurements," *8th AIAA/CEAS Aeroacoustics Conference & Exhibit*, Breckenridge, CO, 2002. https://doi.org/10.2514/6.2002-2470.